Interaction of the spin-flop phase and superconductivity in $DyMo_6S_8$ single crystals

K. Rogacki
Institute of Low Temperature and Structure Research, Polish Academy of Sciences, 50-950 Wroclaw, Poland

E. Tjukanoff* and S. Jaakkola
Wihuri Physical Laboratory, Department of Physics, University of Turku, 20-014 Turku, Finland
(Received 8 December 2000; published 14 August 2001)

Single crystals of $DyMo_6S_8$ are studied by magnetization measurements performed in low magnetic fields and at temperatures below the superconducting transition temperature $T_c = 1.6$ K. Effects have been found at temperatures below $T_N = 0.4$ K, where superconductivity and antiferromagnetic order coexist. These effects reflect the unusual vortex dynamics characterizing the quasistatic magnetization process. The two-stage flux penetration is observed and interpreted as a result of the spin-flop phase developed in the superconducting state. The superconducting coherence length $\xi(0.1\ \mathrm{K}) \simeq 500$ Å and the Ginzburg-Landau parameter $\kappa(0.1\ \mathrm{K}) \simeq 2.5$ have been estimated in the magnetic superconducting state through analysis of the magnetization process. The significant reduction of κ, from 11 obtained just above T_N to about 2.5 below T_N, demonstrates the tendency of the compound to transform from a type-II to a type-I superconductor due to the appearance of long-range magnetic order in the superconducting state.

DOI: 10.1103/PhysRevB.64.094520 PACS number(s): 74.25.Ha, 74.60.Ge, 74.70.Dd

I. INTRODUCTION

Investigation of the interaction between magnetism and superconductivity began about 40 years ago with theoretical and experimental activities appearing simultaneously.[1] The huge interest in the coexistence of these competing effects exploded in the late 1970s with the discovery of two families of magnetic superconductors, the rare-earth-based Chevrel-phases and the rhodium borides.[2] However, for almost two decades the interest has been overshadowed by the high-temperature superconductivity found in copper oxides. The recent discovery of the presence of long-range magnetic order and superconductivity in rare-earth nickel borocarbides [3–8] and Ru-based compounds[9–14] has triggered a series of experiments and inspired a return to the so-called coexistence problem.

Among classic magnetic superconductors, the Chevrel phases have been studied most intensively.[1,15,16] These compounds have been available mainly as polycrystalline materials. However, some interesting features can only be observed for single crystals. One such effect demonstrating the coexistence of and interaction between superconductivity and magnetism is the two-step decrease of the magnetization with increasing external field observed for the antiferromagnetic superconductor $ErRh_4B_4$.[17] This anomaly was explained as a result of the metamagnetic transition in the vortex core and, consequently, the increase of the vortex energy. The magnetic transition in the vortex core seems to create a type of vortices with unique magnetic structure, as considered in detail by Krzyszton.[18,19] Under certain conditions, these vortices may be present in many types of antiferromagnetic superconductors, including the high-T_c cuprites.[20] In this paper, the two-step decrease of the magnetization during the flux penetration process is presented for a single crystal of the Chevrel-phase-type compound $DyMo_6S_8$. Our results confirm the universal character of the unusual behavior of the vortices during the magnetization of the classic antiferromagnetic superconductors in fields close to the first critical field H_{C1}.

$DyMo_6S_8$ is a material with the superconducting transition temperature ranging from 1.6 to 2.2 K for polycrystalline samples.[21–23] The transition from the paramagnetic (PM) to the antiferromagnetic (AFM) state occurs at $T_N = 0.4$ K and is reproducible for good quality samples,[21,24] including single crystals (this work). The crystal structure of $DyMo_6S_8$ can be described as interconnected Mo_6S_8 units and Dy ions. One such unit is a slightly deformed cube where S atoms sit at the corners and Mo atoms (forming a slightly deformed octahedron) are situated at the cube faces. The Mo_6S_8 units are arranged in a simple rhombohedral lattice and the Dy ions are located in the center of the unit cell (are surrounded by eight Mo_6S_8 units), as in other Chevrel phases with rare-earth (RE) ions.[29]

Neutron scattering studies have confirmed the above-mentioned T_N and shown that AFM order is long range with a correlation length greater than 300 Å.[25] The Dy ions form a simple cubic sublattice (with a slight rhombohedral distortion) in which the observed magnetic structure consists of (100) planes with moments of $8.8\mu_B$ alternately parallel and antiparallel to the [111] direction (the rhombohedral axis).[25] Neutron experiments performed at $T = 0.2$ K in an applied magnetic field have demonstrated that ferromagnetic order begins to develop at $H = 200$ Oe,[26] much below the superconducting upper critical field $H_{C2} = 1.2$ kOe.[21] Thus, ferromagnetism coexists with superconductivity in the same manner as antiferromagnetism. For an applied field parallel to the [111] direction (the magnetic easy-axis direction), as in our experiment, the ferromagnetism is spin-flop type.[27] In this work, magnetization measurements were performed to demonstrate the interaction between the spin-flop phase and superconductivity and to study the unusual vortex dynamics in the magnetic state of the AFM superconductor $DyMo_6S_8$.

II. EXPERIMENTAL DETAILS

Single crystals were grown by slow cooling of a melted charge containing a mixture of the $DyMo_6S_8$ and Dy_2S_3 powders. The purity of all materials used for the preparation of the starting powders was better than 99.99%. First, DyS, Mo, and S, with nominal composition $Dy_{1.07}Mo_{6.3}S_8$, were heated at 1000 °C for 5 h in an evacuated quartz ampoule to obtain a Chevrel phase powder. This powder was pressed at 8 bars into a pellet and heat treated in an evacuated molybdenum ampoule for 24 h at 1350 °C. The only impurity phase showed by x-ray analysis was 3% of Mo. The $DyMo_6S_8$ pellet had a residual resistivity ratio equal to 24. This confirms the high quality and homogeneity of the specimen. Then, the pellet was powdered and mechanically mixed with an appropriate amount of the Dy_2S_3 powder. The crystallization process was performed in hermetically sealed molybdenum ampoules cooled from a temperature between 1850 and 1880 °C at the rate of 5–8 °C/h for the first 180 °C. Details of the crystallization procedure are described elsewhere.[28] After many attempts, several single crystals with varied shape and dimension were obtained. Regular cubes with a volume exceeding 0.005 mm^3 appeared only occasionally.

Chemical composition and crystal uniformity were examined using a Hitachi scanning electron microscope equipped with an energy-dispersive x-ray analyzer. Single-crystal x-ray diffraction data were collected at room temperature on a Simens SMART charge-coupled device (CCD) diffractometer. The electron-probe microanalysis of the regular-shaped crystals showed a composition corresponding to the $DyMo_6S_8$ formula. At room temperature, the cell parameters in the rhombohedral lattice were $a_R = 6.452$ Å and $\alpha_R = 89.50°$, and were equivalent for all crystals analyzed. These values are identical to those obtained for polycrystalline materials.[29] The single crystal selected for our experiment showed good stoichiometry and no second phases. It had dimensions of $0.2 \times 0.2 \times 0.2$ mm^3 and a mass $m \simeq 0.05$ mg.

Magnetization was measured with the SHE 330X Series superconducting quantum interference device (SQUID) system with a SQUID sensor installed in the vacuum chamber of the ^{3}He-^{4}He dilution refrigerator. The sensor was thermally anchored to the liquid He bath (4.2 K) and shielded with a Nb tube. Two counterwound pickup coils (each composed of four turns) were made from 0.13-mm-diam Nb-Ti wire and connected to the input coil of the SQUID sensor. The distance between the pickup coils was 15 mm and the coil diameter was 5 mm. Nb-Ti wires leading to the input coil were twisted and shielded with a Pb-Sn tube. The pickup coil assembly was placed in the center of a 10-cm-long superconducting solenoid generating a magnetic field up to 1.5 kOe. Both the coil assembly and the solenoid were fixed to the mixing chamber of the dilution refrigerator. The selected single crystal was glued by GE varnish to the end of a 1.5-mm-diam copper rod and placed in the center of one of the two pickup coils. The other end of the copper rod was screwed to the coil assembly.

This SQUID system, in principle, allows for the measurements of the changes of the magnetization. However, assuming that the sample in the Meissner state demonstrates perfect shielding ($4\pi M = -H$), absolute magnetization values can also be obtained. The perfect shielding was used to calibrate the SQUID system for the magnetization measurements performed with increasing magnetic field for the single crystal in the virgin superconducting state. The crystal was oriented with the magnetic easy axis (the [111] crystallographic triple axis) parallel to the external magnetic field. For this orientation, the demagnetizing factor was assumed to be $k = 1/3$, the same as for a sphere.[30,31] This demagnetizing factor was used to correct magnetic field values; however, the correction is of no importance for our conclusions.

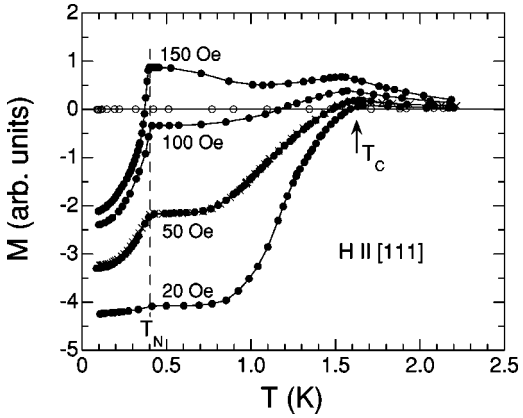

FIG. 1. Magnetization vs temperature at several applied fields for $DyMo_6S_8$ single crystal with the magnetic easy axis oriented parallel to the field direction. The open symbols denote the background results obtained at $H = 0$. Magnetization results obtained from measurements repeated at the same field are marked by $\times$.

III. RESULTS AND DISCUSSION

In Fig. 1, the magnetization measured as a function of temperature is presented for several different applied magnetic fields oriented parallel to the easy axis of the single crystal. At low fields, the transition to the superconducting state is clearly manifested as the smooth change of the magnetization M into diamagnetic values at $T_c \simeq 1.6$ K ($T_c = 1.62$ K for $H = 20$ Oe). This temperature decreases with increasing field, as expected for a superconductor, and reflects the temperature dependence of the upper critical field H_{C2}, below which the resistivity of the single crystal is expected to be equal to zero. For $H > 100$ Oe, the M values below and close to T_c are no longer diamagnetic. However, the resistivity should still be zero and the ac susceptibility should be negative (diamagnetic) as was observed for $DyMo_6S_8$ polycrystalline samples[22] and other magnetic superconductors.[21,32] For these fields, the diamagnetic change of M caused by the superconducting transition is not large enough to compensate the positive M of the Dy ions in the PM state. Thus, the values of M for the sample in the superconducting state depend on the internal magnetic field caused by the applied field and the partially oriented spins of the Dy ions. At lower temperatures, the abrupt change of M is observed at $T_N = 0.4$ K, reflecting the transition to the

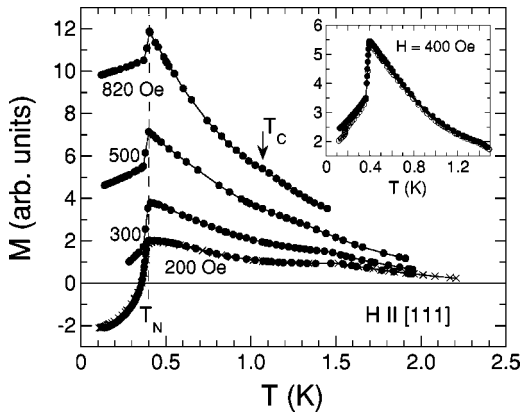

FIG. 2. Magnetization vs temperature at higher fields than in Fig. 1. Magnetization results obtained from measurements repeated at the same field are marked by ×. The inset shows a difference between the dynamic (open symbols) and quasistatic (solid symbols) results (see text).

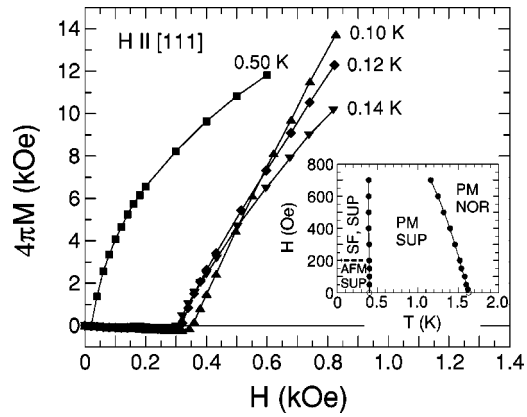

FIG. 3. Magnetization as a function of applied field obtained in the virgin state at several temperatures for $DyMo_6S_8$ single crystal with the magnetic easy axis oriented parallel to the field direction. The inset shows the *H-T* phase diagram with the following series: PM, paramagnetic; NOR, normal; SUP, superconducting; SF, spin flop; and AFM, antiferromagnetic. Two open symbols denote the results obtained by extrapolation. The dashed line was achieved from the neutron diffraction studies (Ref. 26).

AFM state. In this state, the internal field is reduced and *M* can again become negative. At T_N, the change of *M* between the PM and AFM states increases with increasing field as expected.

In Fig. 2, the magnetization measured as a function of temperature is presented for $H \geqslant 200$ Oe. For these fields and below T_N, the single crystal is in the spin-flop (SF) phase, so the observed change of *M*, caused by the transition to the ordered state, decreases significantly with increasing field. The temperature of the magnetic transition is field independent, as expected for an antiferromagnet in low fields. The transition to the superconducting state, appearing as a small kink on the paramagnetic part of the $M(T)$ curve, is still observed, and the results presented in Figs. 1 and 2 can be used to construct the *H-T* phase diagram. At temperatures below T_N, the values of *M* depend slightly on the measuring procedure because of increased flux creep or flux flow effects. For fields higher than 300 Oe, the difference between *M* measured just after the temperature was changed and stabilized (dynamic results) or 1 min later (quasistatic results) is notable. As an example, the difference between the dynamic and static results is presented in the inset of Fig. 2 for $H = 400$ Oe. Note that neither T_c nor T_N depends on the relaxation effects. With the exception of the inset in Fig. 2, all *M* data reported in this paper relate to the quasistatic measurements.

The most interesting results were obtained for *M* measured as a function of applied magnetic field. Figure 3 presents *M* versus *H* at several temperatures below T_N and at 0.5 K. The curves were obtained for the virgin state of the sample. This means that the crystal was cooled to the required temperature from above T_C in zero field and then the field was swept up. The difference between the virgin curves measured in the AFM and PM states is striking and can be understood in terms of the phase diagram shown in the inset of Fig. 3. This diagram, which was constructed by using the results presented in Figs. 1 and 2, is qualitatively similar to the phase diagram obtained for polycrystalline material.[21] At 0.5 K, the sample is in the superconducting and PM states and the change of *M* from negative to positive values takes place at a very low field, just above the first penetration field ($H_{fp} = 10$ Oe) which is the experimental measure of H_{C1}. The large increase (from about 20 to about 300 Oe) of the field at which *M* changes from negative to positive is observed for the sample in the magnetically ordered state. This large increase occurs at temperatures much below T_c and cannot be explained as a result of the temperature dependence of H_{C1}. Thus, it is perceived as a consequence of AFM order appearing in the superconducting state. A similar anomaly, which arises from the fact that the virgin curve was placed out of the magnetization loop, has been observed for the polycrystalline $DyMo_6S_8$ sample; however, this observation has not been interpreted.[24]

The low-field part of the $M(H)$ virgin curves is presented in Fig. 4 to show details concerning flux penetration. This penetration is typical above T_N and proceeds as an unusual

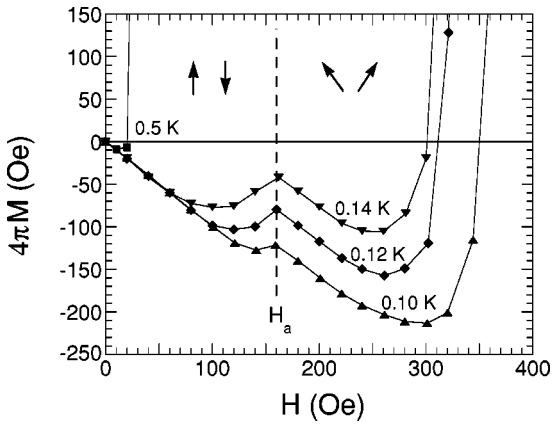

FIG. 4. Details of the magnetization virgin curves presented in Fig. 3. The vertical dashed line marks the field H_a for which the magnetization anomaly appears. The arrows show the possible configuration of the spins of Dy ions in the vortex core.

two-stage process at lower temperatures where AFM order coexists with superconductivity. At low fields the sample is in the Meissner state, i.e., $4\pi M=-H$. When the field increases above H_{fp} ($H_{fp}=120$ and 60 Oe at 0.1 and 0.14 K, respectively), the sample is penetrated by the flux. Then, at higher fields, the penetration process stops unexpectedly, and B in the single crystal is almost constant when the applied field is increased ($\Delta H\simeq-4\pi\Delta M$). This new perfect shielding appears at $H_a=160$ Oe which after correction for demagnetizing effects [$H=(H_a-kB)/(1-k)$, where $k=1/3$] gives the value of 200 and 170 Oe at 0.1 and 0.14 K, respectively. These fields correspond very well to the spin-flop field $H_{SF}=200$ Oe, obtained from neutron diffraction experiments.[26] Thus, we propose the following interpretation of the observed anomaly. When the vortices penetrate the single crystal above H_{fp}, the core and the rest of the vortex are in the AFM phase. However, when the applied field is high enough to force Dy spins to form the SF phase in the vortex core, the vortex energy increases and this will require a higher applied field to push the vortices with the new internal magnetic structure to the sample.[19] Then, with further increase of the applied field, the vortices penetrate the sample more rapidly, the internal magnetic field increases, and the magnetization becomes positive.

In the next part, simple phenomenological considerations are proposed to estimate the number of magnetic ions in the vortex core and, based on that, the superconducting coherence length and the Ginzburg-Landau (GL) parameter for $DyMo_6S_8$ in the AFM superconducting state.

For a local magnetic field lower than the field at which the spin-flop phase occurs, the free energy density of the magnetic superconductor can be expressed as

$$F(H,T)=E_v^0 n+U(n)-BH/4\pi, \tag{1}$$

where E_v^0 is the self-energy of the vortex, n is the vortex density, $U(n)$ describes the interaction energy between the vortices [repulsive interaction means $U(n)>0$], and $BH/4\pi$ reflects the interaction energy between the magnetization and the external field.[33] The transition from the Meissner to a mixed state appears when the external field is equal to $H_{C1}=4\pi E_v^o/\phi_0$, where ϕ_0 is the unit flux. In the mixed state, the magnetic induction is given by the total magnetic flux, $B=\phi_0 n$. Then, the vortex density n is determined by minimizing the free energy (1) with respect to n.

Above H_{SF}, the SF phase develops to reduce the interaction energy between the magnetization and the magnetic field. The SF phase should appear first in the core of the vortex forming the new type of vortices discussed in the former section. The transition to the SF phase results in an increase of the exchange energy between the magnetic spins of RE ions. The increase should be added to the core energy of the vortex:

$$E_v=E_v^0+E_{exch}, \tag{2}$$

where E_{exch} is the increase of exchange energy due to the occurrence of the SF phase in the vortex core. In the first approximation,

$$E_{exch}=\alpha(H-H_{SF})=N_0 e_{exch}, \tag{3}$$

where α is a positive constant, N_0 is the number of Dy ions (spins) in the vortex core, and e_{exch} is the increase of exchange energy per spin due to the SF transition. Then, the free energy in the mixed state for $H>H_{SF}$ is given by

$$\begin{aligned}F(H,T)&=(E_v^0+E_{exch})n+U(n)-\frac{\phi_0 n}{4\pi}(H_{SF}+H-H_{SF})\\&=E_v^0 n+\alpha(H-H_{SF})n+U(n)-\frac{\phi_0 n}{4\pi}H_{SF}\\&\quad-\frac{\phi_0 n}{4\pi}(H-H_{SF})\\&=\left(E_v^0-\frac{\phi_0 H_{SF}}{4\pi}\right)n+\left(\alpha-\frac{\phi_0}{4\pi}\right)(H-H_{SF})n+U(n).\end{aligned} \tag{4}$$

The first term of the final form is negative because $E_v^0=H_{C1}\phi_0/4\pi$ and $H_{SF}>H_{C1}$ for the $DyMo_6S_8$ single crystal. Thus, for H increasing above H_{SF} the vortex density n can stay constant, increase or decrease, depending on α. In our experiment, $n\simeq$const for H changing from 200 to 300 Oe at 0.1 K (after correction for demagnetizing effects), as shown in Fig. 4. For fields in that interval, the single crystal behaves almost as an ideal diamagnet ($\Delta H=-4\pi\Delta M$) and $B\simeq$const (the case $\alpha=\phi_0/4\pi$). Thus, the number of Dy ions in the vortex core can be estimated from the value of α, as shown below.

For H parallel to the easy axis, the increase of the exchange energy due to the SF transition $e_{exch}\simeq\mu_{SF}H_{SF}/2$, where μ_{SF} is the ''on-field'' component of the magnetic moment of the Dy ion in the SF phase. Then, analyzing the shape of the magnetization loops obtained in arbitrary units in high magnetic fields,[24] we evaluate μ_{SF} as 2/3 of the saturation magnetic moment, so $\mu_{SF}\simeq 2\mu_z/3\simeq 6\mu_B$, where $\mu_z=8.8\mu_B$ is the z component of the Dy magnetic moment, as determined by neutron scattering experiments,[25] and μ_B is the Bohr magneton. Then taking the experimental value for $H_{SF}=200$ Oe,[26] we estimate $e_{exch}\simeq 5.6\times10^{-18}$ erg. Now using Eq. (3), with condition $\alpha=\phi_0/4\pi$, and taking the field range for which n is constant ($H-H_{SF}=100$ Oe at 0.1 K, after correction for demagnetizing effects), the number of Dy ions in the vortex core can be calculated from

$$\frac{\phi_0}{4\pi}(H-H_{SF})=N_0 e_{exch} \tag{5}$$

to be $N_0=2.9\times10^{11}$ cm^{-1}. This value corresponds to the core diameter $d(0.1\text{ K})\simeq 1000$ Å. Assuming $d\simeq 2\xi$, the superconducting coherence length $\xi(0.1\text{ K})\simeq 500$ Å is obtained. In our experiment $B\simeq$const$=100$ G (at 0.1 K), which corresponds to $n\simeq 4.8\times10^8$ cm^{-2} and to the distance between vortices $a\simeq 7000$ Å for a triangle lattice.

The coherence length can also be estimated from the simple formula $H_{C2}=\phi_0/2\pi\xi^2$. For our $DyMo_6S_8$ single crystal, $H_{C2}=900$ and 1100 Oe at 0.1 and 0.7 K, respec-

tively, and consequently, $\xi \simeq 600$ and 550 Å which correlates very well with the value obtained above. Encouraged by this result, we use the GL relation between H_{C1} and H_{C2}, $(H_{C1}/H_{C2}) = (\pi \ln\kappa / 4\sqrt{3}\kappa^2)$,[34] to estimate the G-L parameter $\kappa(0.7\ \mathrm{K}) \simeq 11$ for $H_{C1} = H_{fp} \simeq 10$ Oe (see Fig. 4) in the nonmagnetic superconducting state. Then, accepting above-evaluated $\xi(0.7\ \mathrm{K}) \simeq 550$ Å we obtain the penetration depth $\lambda(0.7\ \mathrm{K}) \simeq 6000$ Å. The GL relation between the lower and upper critical fields is generally valid for superconductors with large κ and, therefore, cannot be applied for our sample in the AFM superconducting state. In that state, the H_{C1}/H_{C2} ratio is considerably reduced (at 0.1 K, $H_{C1} = H_{fp} \simeq 100$ Oe and $H_{C2} = 900$ Oe) which requires the reduction of κ, possibly even below 2. However, to estimate κ below T_N, we can assume that in the SF phase λ is reduced to the value of order $(\lambda l)^{1/2}$, where l is the magnetic interaction length.[35] For $DyMo_6S_8$, [26] $l \simeq 300$ Å and, using the above obtained value $\lambda(0.7\ \mathrm{K}) \simeq 6000$ Å, we obtain in the magnetically ordered state $\lambda(0.1\ \mathrm{K}) \simeq 1300$ Å. Comparing the new estimated $\lambda(0.1\ \mathrm{K})$ with the distance between vortices, $a \simeq 7000$ Å, we see that at fields where the magnetization anomaly occurs the vortices can be considered as isolated.

The reduction of λ, observed in the AFM state, leads to a strong compression of the quantized flux and results in a considerable decrease of the GL parameter from $\kappa(0.7\ \mathrm{K}) \simeq 11$ to $\kappa(0.1\ \mathrm{K}) \simeq 2.5$. Both of the values of κ may be underestimated because in calculations we used H_{fp} instead of H_{C1} and $H_{fp} \geqslant H_{C1}$ (real H_{C1} values are usually not known). However, we can conclude that the appearance of the SF phase in the superconducting state forces the type-II magnetic superconductor, even when it has a large κ, to become a type-I superconductor as predicted theoretically.[36,37] One possible reason for this effect is the attractive force between the vortices caused by the current inversion in some portion of the vortex with the special magnetic structure. The current inversion seems to be the direct consequence of the quantization of the total flux of a single vortex, which in a magnetic superconductor is the sum of the spin and current contribution.[36]

IV. CONCLUSION

The single crystals of $DyMo_6S_8$ were successfully grown using the slow cooling of a melted charge closed in hermetically sealed molybdenum ampoules. The crystals were pure, homogenous, and large enough to be used for studying some subtle effects accompanying the magnetization of the antiferromagnetic superconductor. For a crystal with the magnetic easy axis oriented parallel to the external field, the unusual vortex behavior was observed below T_N for the initial magnetization process. This behavior, which is two-stage flux penetration, was interpreted as the consequence of the spin-flop phase appearing in the vortex core. Based on this observation and analyzing the free energy of the magnetic superconductor, the superconducting coherence length and the GL parameter κ were estimated in the magnetic superconducting state. In this state, κ is too small to be obtained by applying the simple GL formulas. The large reduction of κ observed below T_N gives evidence that with decreasing temperature the antiferromagnetic superconductor tries to transform from a type-II (with a large κ) to a type-I superconductor. This transformation can be explained as a result of the attractive force between the vortices, possibly due to the current inversion in some portion of the vortex.

ACKNOWLEDGMENTS

The authors acknowledge valuable discussions with T. Krzyszton, P. Tekiel, and R. Laiho. This work was supported by the Polish State Committee for Scientific Research within Project No. 2 P03B 125 19 and by the Wihuri Foundation, Finland.

*Present address: Laboratory of Electronics, Department of Applied Physics, University of Turku, 20014 Turku, Finland.

[1] For review, see M. B. Maple and Ø. Fisher, in *Superconductivity in Ternary Compounds II*, edited by M. B. Maple, and Ø. Fisher (Springer-Verlag, Berlin, 1982), Chap. 1 and references therein.

[2] For reviews, see *Superconductivity in Ternary Compounds I, II*, edited by M. B. Maple, and Ø. Fisher (Springer-Verlag, Berlin, 1982); M. B. Maple, J. Magn. Magn. Mater. **31-34**, 479 (1983); K. Machida, Appl. Phys. **35**, 193 (1984); S. L. Kakani and U. N. Upadhyaya, J. Low Temp. Phys. **70**, 5 (1988); M. B. Maple, Physica B **215**, 110 (1995).

[3] R. Nagarajan, C. Mazumdar, Z. Hossain, S. K. Dhar, K. V. Gopalakrishnan, L. C. Gupta, C. Godart, B. D. Padalia, and R. Vijayaraghavan, Phys. Rev. Lett. **72**, 274 (1994).

[4] R. J. Cava, H. Takagi, B. Batlogg, H. W. Zandbergen, J. J. Krajewski, W. F. Peck, Jr., R. B. van Dover, R. J. Felder, T. Siegrist, K. Mizuhashi, J. O. Lee, H. Eisaki, S. A. Carter, and S. Uchida, Nature (London) **367**, 146 (1994).

[5] R. J. Cava, H. Takagi, H. W. Zandbergen, J. J. Krajewski, W. F. Peck, Jr., T. Siegrist, B. Batlogg, R. B. van Dover, R. J. Felder, K. Mizuhashi, J. O. Lee, H. Eisaki, and S. Uchida, Nature (London) **367**, 252 (1994).

[6] T. Siegrist, H. W. Zandbergen, R. J. Cava, J. J. Krajewski, and W. F. Peck, Jr., Nature (London) **367**, 254 (1994).

[7] J. W. Lynn, S. Skanthakumar, Q. Huang, S. K. Sinha, Z. Hossain, L. C. Gupta, R. Nagarajan, and C. Godart, Phys. Rev. B **55**, 6584 (1997).

[8] For review, see P. C. Canfield, P. L. Gammel, and D. J. Bishop, Phys. Today **51(10)**, 40 (1998).

[9] L. Bauernfeind, W. Widder, and H. F. Braun, Physica C **254**, 151 (1995).

[10] I. Felner, U. Asaf, Y. Levi, and O. Millo, Phys. Rev. B **55**, R3374 (1997).

[11] I. Felner, U. Asaf, S. Reich, and Y. Tsabba, Physica C **311**, 163 (1999).

[12] C. Bernhard, J. L. Tallon, Ch. Niedermayer, Th. Blasius, A. Golnik, E. Brücher, R. K. Kremer, D. R. Noakes, C. E. Sronach, and E. J. Ansaldo, Phys. Rev. B **59**, 14 099 (1999).

[13] D. J. Pringle, J. L. Tallon, B. G. Walker, and H. J. Trodahl, Phys. Rev. B **59**, R11 679 (1999).

[14] A. Fainstein, E. Winkler, A. Butera, and J. Tallon, Phys. Rev. B **60**, R12 597 (1999).
[15] P. Burlet, J. Flouquet, J. L. Genicon, R. Horyn, O. Pena, and M. Sergent, Physica B **215**, 127 (1995).
[16] B. Wolf, J. Molter, G. Bruls, B. Lüthi, and L. Jansen, Phys. Rev. B **54**, 348 (1996).
[17] H. Iwasaki, M. Ikebe, and Y. Muto, Phys. Rev. B **33**, 4669 (1986).
[18] T. Krzyszton, J. Magn. Magn. Mater. **15-18**, 1572 (1980).
[19] T. Krzyszton, Phys. Lett. **104A**, 225 (1984).
[20] T. Krzyszton, Physica C **294**, 47 (1998).
[21] M. Ishikawa and Ø. Fischer, Solid State Commun. **24**, 747 (1977).
[22] H. C. Freyhardt, K. Winzer, and W. Schroter, J. Phys. (Paris), Colloq. **39**, C6-369 (1978).
[23] L. D. Woolf, M. Tovar, H. C. Hamaker, and M. B. Maple, Phys. Lett. **74A**, 363 (1979).
[24] M. Ishikawa and J. Muller, Solid State Commun. **27**, 761 (1978).
[25] D. E. Moncton, G. Shirane, W. Thomlinson, M. Ishikawa, and Ø. Fischer, Phys. Rev. Lett. **41**, 1133 (1978).
[26] W. Thomlinson, G. Shirane, D. E. Moncton, M. Ishikawa, and Ø. Fischer, J. Appl. Phys. **50**, 1981 (1979).
[27] W. Thomlinson, G. Shirane, J. W. Lynn, and D. E. Moncton, in *Superconductivity in Ternary Compounds II*, edited by M. B. Maple and Ø. Fisher (Springer-Verlag, Berlin, 1982), Chap. 8.
[28] R. Horyn, O. Pena, C. Geantet, and M. Sergent, Supercond. Sci. Technol. **2**, 71 (1989).
[29] Ø. Fischer, Appl. Phys. **16**, 1 (1978).
[30] V. V. Schmidt, *The Physics of Superconductors* (Springer-Verlag, Berlin, 1997), Chap. 1.
[31] R. B. Goldfarb, M. Lelental, and C. A. Thompson, in *Magnetic Susceptibility of Superconductors and Other Spin Systems*, edited by R. A. Hein *et al.* (Plenum Press, New York, 1991), pp. 49–80.
[32] M. Ishikawa and Ø. Fischer, Solid State Commun. **23**, 37 (1977).
[33] P. G. de Gennes, *Superconductivity of Metals and Alloys* (Benjamin, New York, 1966), Chap. 3.2.
[34] M. Tinkham, *Introduction to Superconductivity* (Krieger, Melbourne, FL, 1975), Chap. 5.3.
[35] P. Fulde, and J. Keller, in *Superconductivity in Ternary Compounds II*, edited by M. B. Maple, and Ø. Fisher (Springer-Verlag, Berlin, 1982), Chap. 9.3.
[36] M. Tachiki, H. Matsumoto, and H. Umezawa, Phys. Rev. B **20**, 1915 (1979).
[37] H. Matsumoto, R. Teshima, H. Umezawa, and M. Tachiki, Phys. Rev. B **27**, 158 (1983).